Multi-chamber tire concept for low rolling-resistance

Aldhufairi, Hamad; Essa, Khamis; Olatunbosun, Oluremi

DOI:
10.4271/06-12-02-0009

Document Version
Peer reviewed version

Citation for published version (Harvard):
Aldhufairi, H, Essa, K & Olatunbosun, O 2019, 'Multi-chamber tire concept for low rolling-resistance', *SAE International Journal of Passenger Cars - Mechanical Systems*, vol. 12, no. 2, 06-12-02-0009, pp. 111-126. https://doi.org/10.4271/06-12-02-0009

Multi-chamber Tire Concept for Low Rolling-Resistance

Hamad Sarhan Aldhufairi[1], Khamis Essa[1] and Oluremi Olatunbosun[1]

[1] Department of Mechanical Engineering, University of Birmingham, Birmingham, B15 2TT, UK

Abstract:

Rolling-resistance is leading the direction of numerous tire developments due to its significant effect on fuel consumption and CO2 emissions considering the vehicles in use globally. Many attempts were made to reduce the rolling-resistance but with no gain or limited success due to the tire complexity and the trade-offs. This paper investigates the concept of multiple chambers inside the tire as a potential alternative solution for reducing the rolling-resistance. To accomplish that, novel multi-chamber designs were introduced and numerically simulated through finite-element (FE) modeling. The FE models were compared against a standard design as the baseline. The influences on rolling-resistance, grip, cornering, and mechanical comfort were studied. The multi-chambers tire reduced rolling-resistance considerably with acceptable trade-offs. Independent air volumes isolating tread from sidewalls would maintain tire's profile effectively. Different air concentration across tire's chambers gave the tire extended versatility. Rolling non-uniformity depends upon inner-chambers' stability, sidewalls' flexibility and tire/chamber(s) integration.

Keywords:

Multi-chambers Tire; Surface-Based Fluid Cavity; Rolling-Resistance; Finite Element Modeling; Tire Structural Design; Inflation Air

1. Introduction:

The rolling-resistance is interpreted as the losses in the tire's mechanical energy (i.e., heat dissipation) during rolling for a distance on the road. For a straight steady-state rolling on a flat road, the primary source for rolling-resistance is the material hysteresis damping. This source is accountable for 80-95% of the tire's rolling-resistance followed by secondary sources; the aerodynamic drag (i.e., 0-15%) and the tire/road friction (i.e., 5%) [1]. This paper will mainly focus on the rolling-resistance due to hysteresis induced by tire deformation during rolling (i.e., tire's internal losses).

Although hysteresis is needed for tire's grip and cushion, generally, the rolling-resistance is an unwanted phenomenon because it can be liable for up to 20-30% of vehicle's fuel consumption according to the driving conditions and hence a large portion of CO2 emissions [2, 3]. Due to the tire complexity, reducing tire's rolling-resistance can be challenging because of the severe compromises it may have with other essential features like grip and cushioning [1].

Multi-chambers tire concept can be seen as a potential alternative solution to reducing rolling-resistance without negatively compromising other core features. Several multi-chambers tire mechanisms are available publicly as patented designs that are not tested or verified [4, 5]. Many of those patents were introduced to secure the beads seating, improve the airtight sealing and handle run-flat [6-10]. Commonly, inner tubing divided by radial-walls and annular dual to triple chambers arranged either side-by-side or concentrically were used. However, questions are raised concerning those designs' feasibility, manufacturability, and addressability of the diverse driving requirements since those patents address individual requirements only with no validations provided.

Other patents were presented to improve the off-road gripping utilizing either concentric annular chambers or detachable annular shoe-casing with built-in chambers [11-13]. Both Merz et al. [14] and Lambe [15] claimed in their patents that fuel economy and cushioning can be improved using annular and concentric dual-chambers; with a lower pressure inner-chamber and a higher pressure outer-chamber. However, this claim can be challenged as it may weaken tire's grip, beads seating, and vehicle stability. The inventors did not provide any empirical or analytical evidence supporting such a claim.

For the tire industry, Coyote [16] introduced an internal pneumatic bead-lock that can transform the standard tire into annular and concentric dual-chambers with higher pressure inner-chamber for supporting beads seating and run-flat cases and lower pressure outer-chamber for off-road gripping. Independently, both Goodyear [17] and Bridgestone [18] introduced a future design concept of an annular multi-chambers tire for better stability, comfortability, and fuel economy through changing chambers' pressures independently and differently. Both manufacturers are striving to develop their conceptual designs into more practical oriented designs.

Kubba [19] investigated a four-chambers prototype experimentally for rolling-resistance and cornering as a part of an unfinished project by Fusion Innovation [4]. In these experiments, he demonstrated that more than one cavity chamber could have an impact on lowering the rolling-resistance. His work included developing an FE model using Abaqus/standard that was limited to predicting the quasi-static characteristics and the cornering lateral forces to an extent. The model failed to predict the rolling-resistance and the cavity chambers behavior because no air/structure interaction was considered.

From the literature above, it can be concluded that there are little and superficial findings on the subject of multi-chambers tire for low rolling-resistance as it is an un-ripened research field at designing stage and lab prototyping with no practical application yet. To the author's knowledge, there are on-going researches in this field which are confidential and mainly belong to automobile and tire institutions. Further research and in-depth investigations, on an analytical and empirical basis, are needed to be carried out. There are many research needs to be investigated including, but not limited to, the effects of chambers' structure, cavity volumes, inflation settings, air/structure interaction, and air-flow pattern(s).

In this context, this paper examines the cavity design of pneumatic multi-chambers tire and its role on rolling-resistance and any trade-offs with other features related to grip, cornering and mechanical comfort under different loadings and working pressures. To meet this aim, the rolling-resistance due to the internal losses of tire's structure only will be assessed to study the effect of the tire chambers structure. Three different novel designs of multi-chambers tire were evaluated through experimentally validated Abaqus/Explicit FE model and compared against a standard (baseline) tire. The developed FE model(s) treats the tire's chambers inside as surface-based fluid cavities to represent the global cavity-air and account for the air/structure interaction.

2. Experimental Work:

A conventional 225/55 R17 radial tire was adopted for this study in Figure 1(B) to use as a baseline (standard) tire and to validate the FE modeling. At a later stage, this standard tire was modified from having a single cavity chamber into having dual (concentric) annular chambers, in Figure 1(C), by fitting an internal bead-lock chamber supplied by Coyote [16] in

Figure 1(C-1) into the tire's main chamber in Figure 1(C-2). This step aims to validate the FE modeling capability to simulate the multi-chambers tire behavior correctly. The bead-lock chamber comes in a standardized size and was not especially made for the investigated tire. This had some implications on the developed dual-chambers tire like imposed increase in weight and limited operation range, especially the applied loadings and inflation pressures, to avoid damaging the tire's chambers.

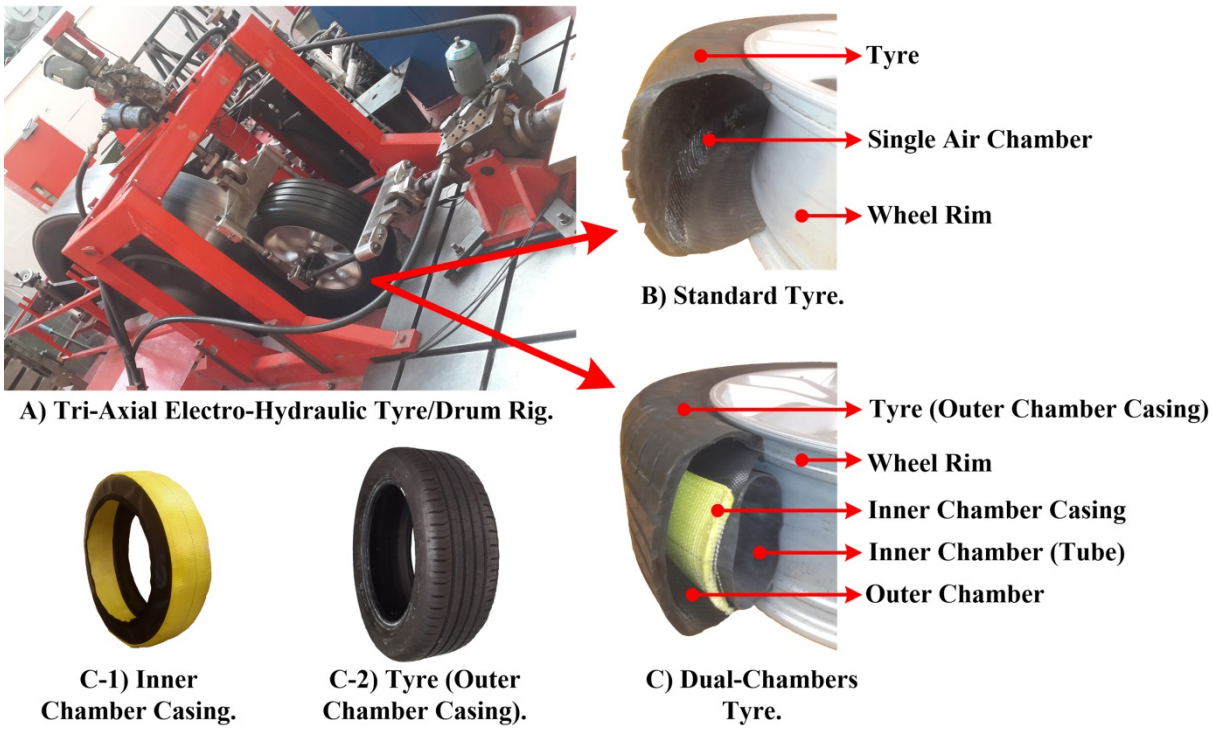

Figure 1. (A) Tire/Drum Rig Set-up of (B) Standard Tire and (C) Dual-Chambers Tire.

2.1 Quasi-Static Testing:

Three quasi-static tests were conducted on both the standard and dual-chambers tires to study several physical features related to rolling-resistance, grip, and mechanical comfort. These tests are used as a first stage validation of the FE modeling. The first test involved measuring the change in the outer tire's cross-sectional profile under different inflation pressures, as in Table 1, at the tread-center and the sidewall outermost point through 3D laser scan using

"Faro Edge ScanArm". Since it is a contact-less test, a wide inflation range was used for the "standard tire" to validate the FE prediction. For the "dual-chambers tire", the inner-chamber was fixed at a high pressure to support beads seating and subsequent chamber(s) while the outer-chamber was set at 180 KPa as a minimum to avoid an inside collision between the chambers and at 240 KPa as a maximum to prevent wrinkling in the inner-chamber.

Table 1. Inflation Pressure Conditions.

Test Type	No	Standard Tire (KPa)	Dual-Chambers Tire (KPa)	
			Inner-Chamber	Outer-Chamber
Outer Cross-Sectional Profile	1	160	280	180
	2	200	280	200
	3	240	280	220
	4	280	280	240
Static Vertical Stiffness	1	180	280	180
	2	200	280	200
	3	220	280	220
	4	240	280	240
	5	260		

For the second test, see Figure 1(A), a "tri-axial electro-hydraulic tire/drum rig" was used to quasi-statically load the tire vertically against the drum at a fixed displacement (i.e., 15mm), under different inflations as in Table 1, while recording the vertical reaction force generated at the wheel center. The "vertical static stiffness" is calculated as the gradient of the reaction-force over the displacement. In Table 1, since it is a contact test, a more practical inflation range was chosen to avoid damaging the tire.

In the third test, the "tire/drum rig" was utilized to quasi-statically push the tire vertically against the drum under different vertical loads (i.e., 1, 2, 3 and 4 KN) and fixed inflation (i.e., Standard=220KPa and Dual-Chambers=Inner (280KPa), Outer (220KPa)). During such test, the tire contact-patch area was captured by spraying the contact-patch with black-ink and

having it imprints on a white A4-paper laid on the drum surface. The footprint area was calculated using image-processing similar to Wei [20].

2.2 Dynamic Testing:

Two rolling tests were done using the "tri-axial electro-hydraulic tire/drum rig" on both the standard and dual-chambers tires to study rolling-resistance, non-uniformity and corner-handling. These tests are used as a second stage validation of the FE modeling.

Table 2. Straight Free-Rolling Conditions.

	Rolling Velocity (Km/h)	**Inflation Pressure (KPa)**	**Vertical Load (KN)**
Standard Tire	30	220	1, 2, 3 and 4
Dual-Chambers Tire	30	Inner=280 , Outer=220	1, 2, 3 and 4

For the first test, the tire was configured to run at the straight steady-state and free-rolling conditions in Table 2. Since this paper's goal is to assess the rolling-resistance due to the tire's internal losses alone, free-rolling cases on a smooth contact-drum were performed to remove the impact of acceleration, deceleration and road roughness on the tire's rolling-resistance. Similarly, the tire was set to roll at a constant low velocity to eliminate the influence of aerodynamic drag on the tire's rolling-resistance. During this test, two parameters were calculated. First, similar to [21], the "rolling-resistance" was determined by measuring the longitudinal force at the wheel-spindle and then calculating the energy dissipated per unit-distance. Secondly, for tire uniformity, the variations in both the vertical and lateral forces at the wheel-spindle were measured similar to Michelin [22].

Typically, the uniformity test is used to test newly manufactured tires for any manufacturing imperfections causing non-uniformities in the rolling tire's structure that undermine the ride

comfort [23]. However, in this paper, the manufacturing imperfections are assumed negligible as the investigated tire is a passed end-product and the FE tire model has perfectly symmetrical geometry and mass distribution around its rotational axis. In this respect, the tire's uniformity can indicate the deformational level in the tire's profile, due to the chamber(s) structural design, and hence the mechanical comfort for perfectly smooth flat-runway. Nevertheless, for real road, the ride comfort will be assessed based on tire's vertical static stiffness.

The second test involved measuring the lateral force at the wheel-spindle while the tire is free-rolling, under different slip angles from 1 to 5 degrees respectively, at 3KN vertical load, a steady-state velocity of 10Km/h, and fixed inflation (i.e., Standard=220KPa and Dual-Chambers=Inner (280KPa), Outer (220KPa)).

3. FE Model Development:

The same tire was used throughout the whole study but with different cavity chamber(s) designs. Abaqus 6.13 was used to develop FE tire models. To account for the tire mechanical behavior in FE, the relevant rubber and reinforcement samples were extracted from the tire structure and tested for the associated hyperelastic, viscoelastic and elastic properties similar to Aldhufairi and Essa [21]. The adopted material models can be found in Table 3 for the associated rubber parts. The reinforcements' elasticity of steel-belts and beads as steel, cap-plies as polyamide, and carcass as polyester were incorporated into the FE model-tree.

Table 3. Material Model(s) Coefficients.

Model's Type	Model's Coefficients	Rubber Sections		
		Tread	Sidewall	Apex
Hyperelastic (Yeoh)	C10	0.641	0.386	0.789
	C20	-0.074	-0.035	-0.155

	C30	0.031	0.009	0.152
Viscoelastic (Power Law Strain Hardening PRF (Parallel Rheological Framework))	SR1	0.396	0.123	0.0001
	SR2	0.031	0	0.394
	SR3	0.007		0.036
	A1	3.869	0.755	0.163
	n1	4.044	2.715	1.050
	m1	-0.650	-0.132	-0.011
	A2	0.304	0.038	1.499
	n2	2.769	1.223	6.496
	m2	-0.007	-0.330	-0.348
	A3	0.364		0.049
	n3	1.213		3.142
	m3	-0.0004		-0.0004

The medium inside the tire chambers were treated as surface-based fluid cavities, modeled by volume elements, to closely simulate the global cavity-air behavior as an ideal gas. This is since it conforms to the key assumptions of kinetic theory for ideal gases [24-26]. In the dual-chambers case, the elasticity of the inner-chamber housing's top as fabric and sides as polyvinyl-chloride (PVC) was incorporated into the relevant FE model. For the other multi-chambers cases, the inner-chambers' walls and its reinforcements had the same properties as the tire's sidewall and carcass respectively.

A detailed geometry of the tire 2D cross-section was captured using an image-processing technique, similar to Yang [27], and imported to Abaqus as a CAD file to build-up a 2D axisymmetric FE model of the tire as shown in Figure 2 (A) for the standard tire and (B) for the dual-chambers one. A pattern-less tread was drawn to eliminate hourglass modes where "patterns" have a negligible effect on rolling-resistance [1, 28-30]. The rubbery parts were presented as solid elements (CGAX4R) and the reinforcements as surface elements (SFMGAX1) implanted inside the related rubbery parts. The tire's wheel was presented through a rigid-body definition linking the wheel center node to the tire/wheel contact nodes.

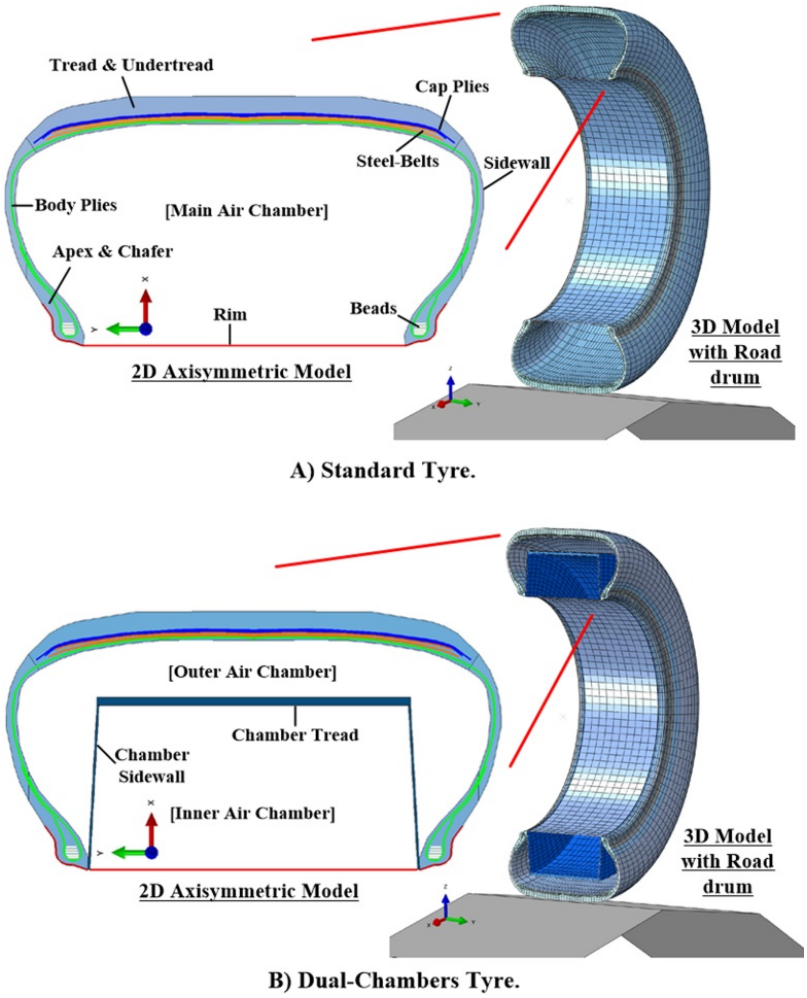

Figure 2. FE Models of (A) Standard Tire and (B) Dual-Chamber Tire.

For the other multi-chambers cases, the inner-chambers walls' reinforcements were laid-up radially similar to the tire's carcass. An additional reinforcement layer was added circumferentially to every wall that was parallel to the tire's tread.

The 2D axisymmetric model was revolved creating a full 3D model, in Figure 2, using the "symmetric model generation" and "symmetric results transfer" procedures available in Abaqus/Standard. An "input" file was created to include the model data, an analytical rigid-surface drum definition, and the necessary analysis steps to simulate the tire's inflation, vertical loading and free-rolling conditions isothermally. The respective tire's mass and

inertia were accounted for using point-mass element paired with rotary-inertia element at the tire center node. The tire analysis was performed through Abaqus/Explicit since the viscoelastic PRF model is not supported with Abaqus/Standard and to account for the non-linear dynamic behavior properly as illustrated in a previous work [21].

4. FE Model Validation:

For the quasi-static behavior, the FE outputs, for both standard and dual-chambers tires, illustrated a good match with the experiments. In Table 4, as inflation pressure goes-up, the tire's tread was pushed outward while the sidewalls were pulled slightly inward to achieve a taller and thinner profile. Similar trends can be found in Yang [27] and Wei [20] works.

Table 4. Cross-Sectional Profile Displacement.

	Inflation Pressure (KPa)		Tread-Centre (mm)		Sidewall Outermost (mm)	
			FE	Experiment	FE	Experiment
Standard Tire	160		1.857	1.881	1.305	1.326
	200		2.362	2.475	1.269	1.250
	240		2.914	3.045	1.188	1.159
	280		3.500	3.480	1.141	1.112
Dual-Chambers Tire	Inner	Outer				
	280	180	2.105	2.585	1.139	1.185
	280	200	2.362	2.796	1.081	1.119
	280	220	2.632	3.047	1.060	1.108
	280	240	2.914	3.190	1.063	1.071

In Figure 3 (A), the increase in the inflation pressure made the tire stiffer as more air molecules were filling the tire cavity to lift-up the vertical load. Similar findings were reached by Lee et al. [31] and Wei [20]. Both standard and dual-chambers tires had almost similar stiffness for the same pressure of the standard tire and the outer-chamber of the dual-chambers tire.

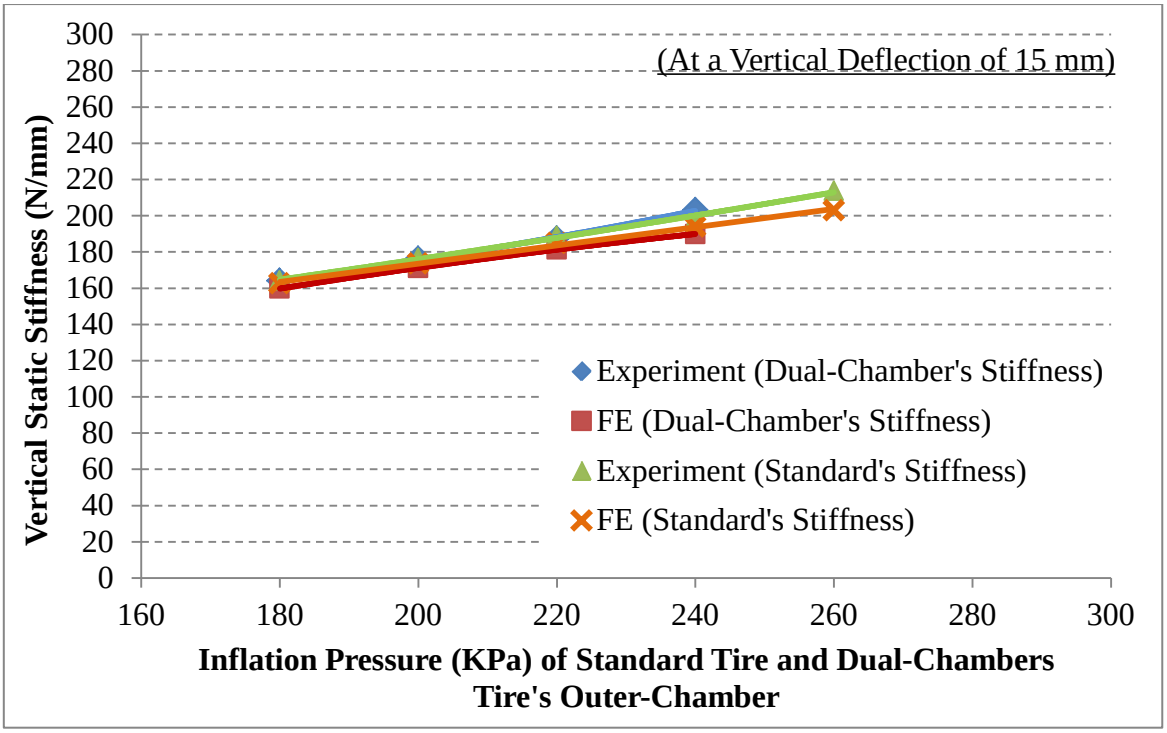

A) Vertical Static Stiffness.

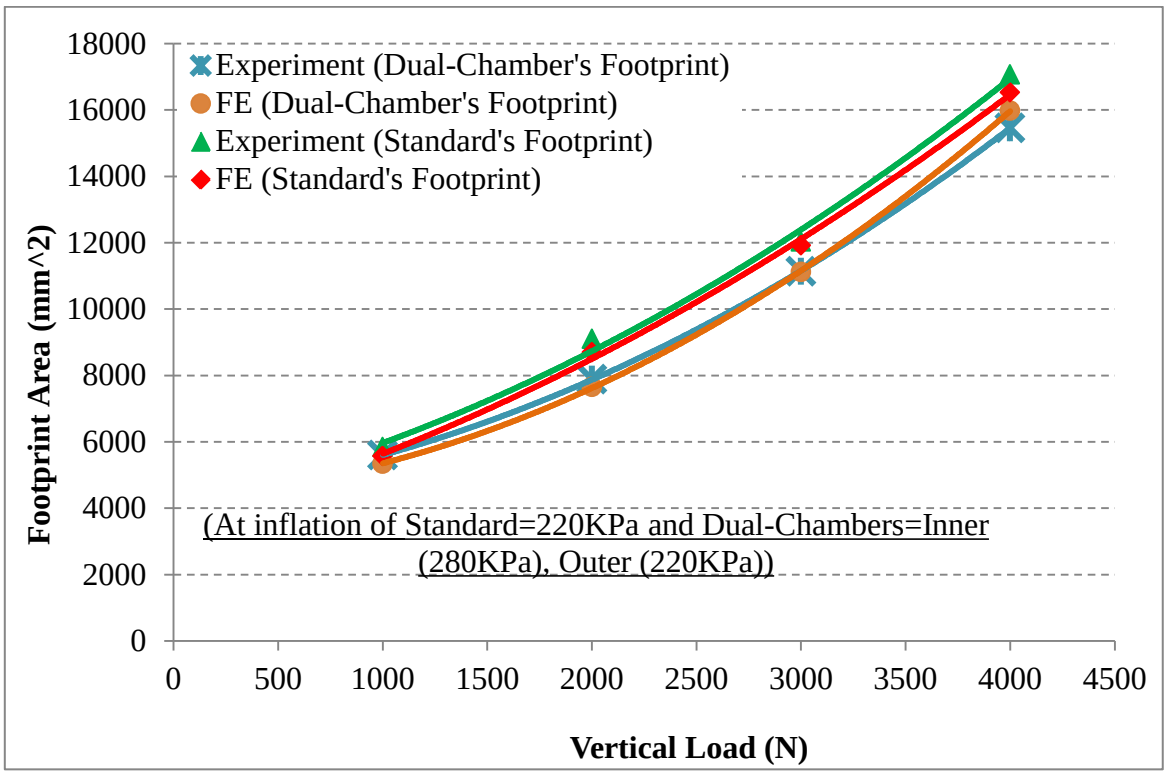

B) Footprint Area.

Figure 3. Tire's Quasi-Static Behavior for (A) Vertical Stiffness and (B) Footprint.

In Figure 3 (B), the standard and dual-chambers tires showed a close footprint area with the dual-chambers having slightly lesser areas. Larger areas were acquired with the increase in the vertical loading which would further compress the inflation-air leading to more tire deformation at the contact-patch. Hoever [32] and Hernandez et al. [33] pointed-out the same outcomes.

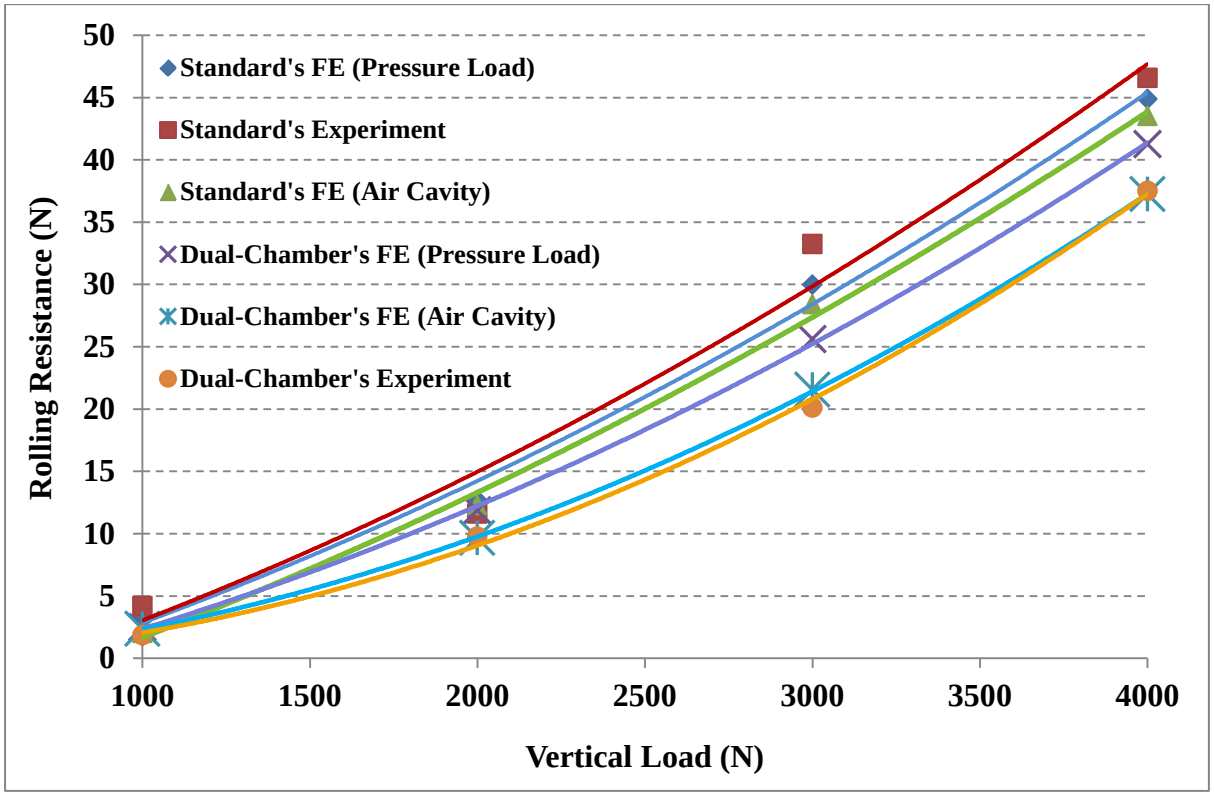

Figure 4. Rolling-Resistance against Vertical Load.

For the dynamical behavior, a good agreement between the FE and the experiments were noted. In Figure 4, the rolling-resistance is nearly linearly proportional to the vertical loading in line with others' works [33, 34]. This is as the higher the load, the larger the tire deformation would be at the contact-patch. In FE, for cavity behavior consideration in rolling-resistance prediction, a comparison was made between applying a "distributed pressure load" over the inner-walls and treating the tire's chamber(s) as filled with "fluid cavity volume" representing air as an ideal gas. No difference was observed in the standard

tire. For the dual-chambers case, the air-cavity method was more accurate in predicting the rolling-resistance than the pressure load method.

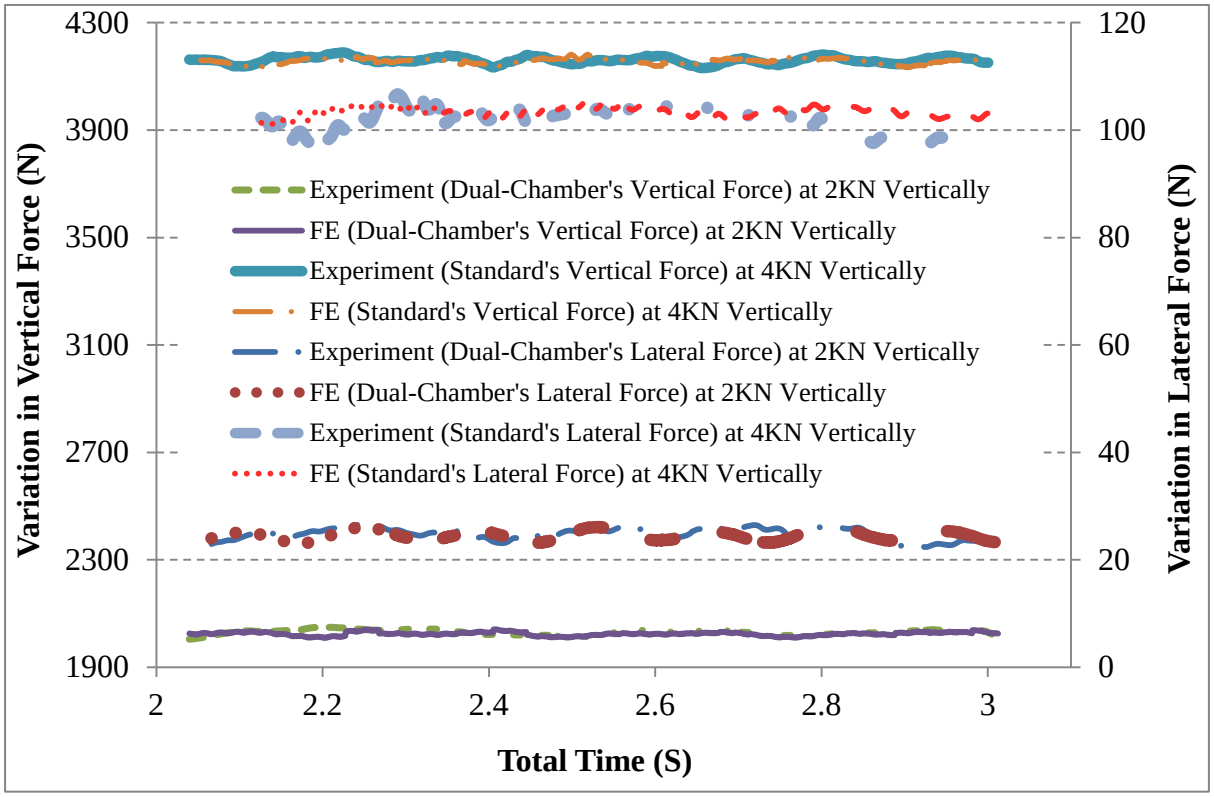

Figure 5. Variations in Axial Forces.

In Figure 5, for tire uniformity, after data low-pass filtration, a reasonable match was achieved between the FE and the experiments with slight differences that could be due to tolerable manufacturing imperfections in the real tire. The cornering performance, in Figure 6, was found to follow the same pattern as the literature [20, 27, 35]. The dual-chambers tire illustrated marginally lower lateral forces.

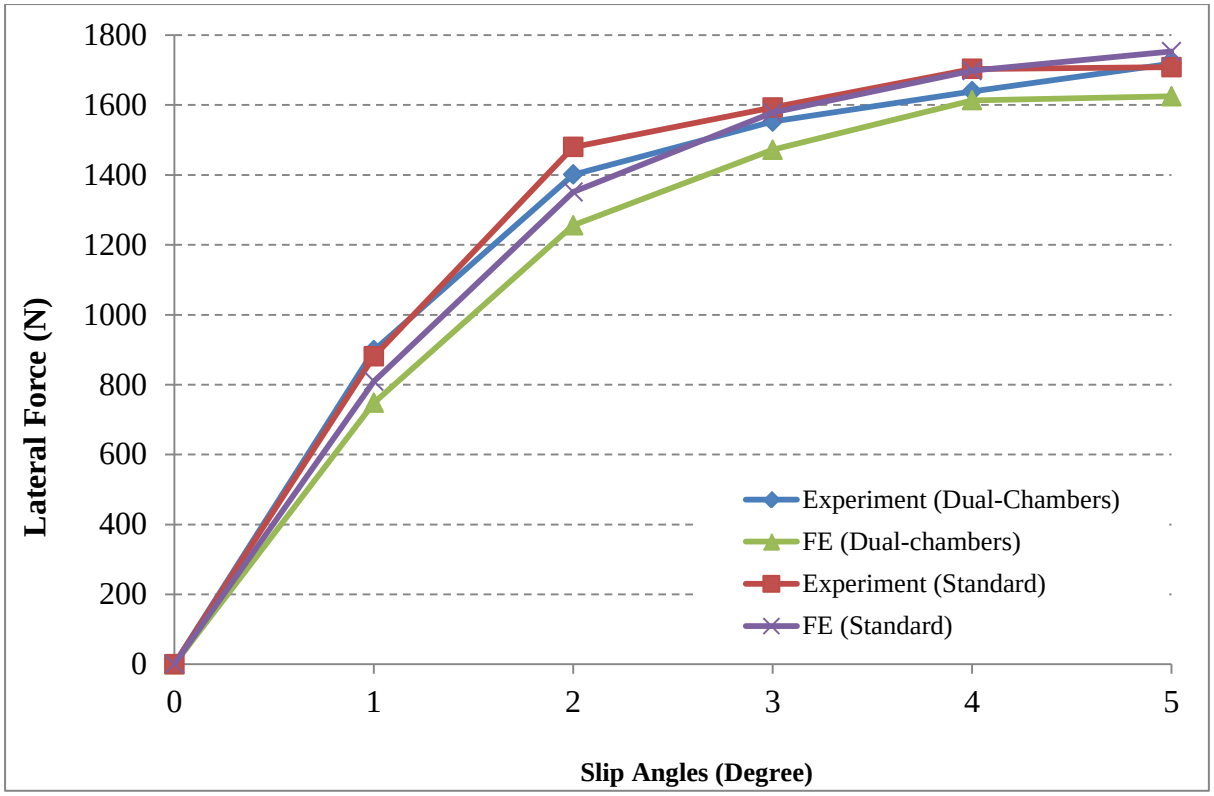

Figure 6. Cornering Lateral Forces.

Taken altogether, as in Figure 7 for example, the dual-chambers solution can offer a reduction of over 10% in rolling-resistance depending on the rolling condition. Such an improvement lies mainly due to the decrease in the dual-chambers' radial non-uniformity which means lesser deformational hysteresis losses. As per the kinetic theory of gases, this is possible as the dual-chambers' outer-chamber provides a smaller space for the cavity air to travel, re-collide and establish pressure again more quickly to support tread's profile without causing violent and large air movement inside the tire.

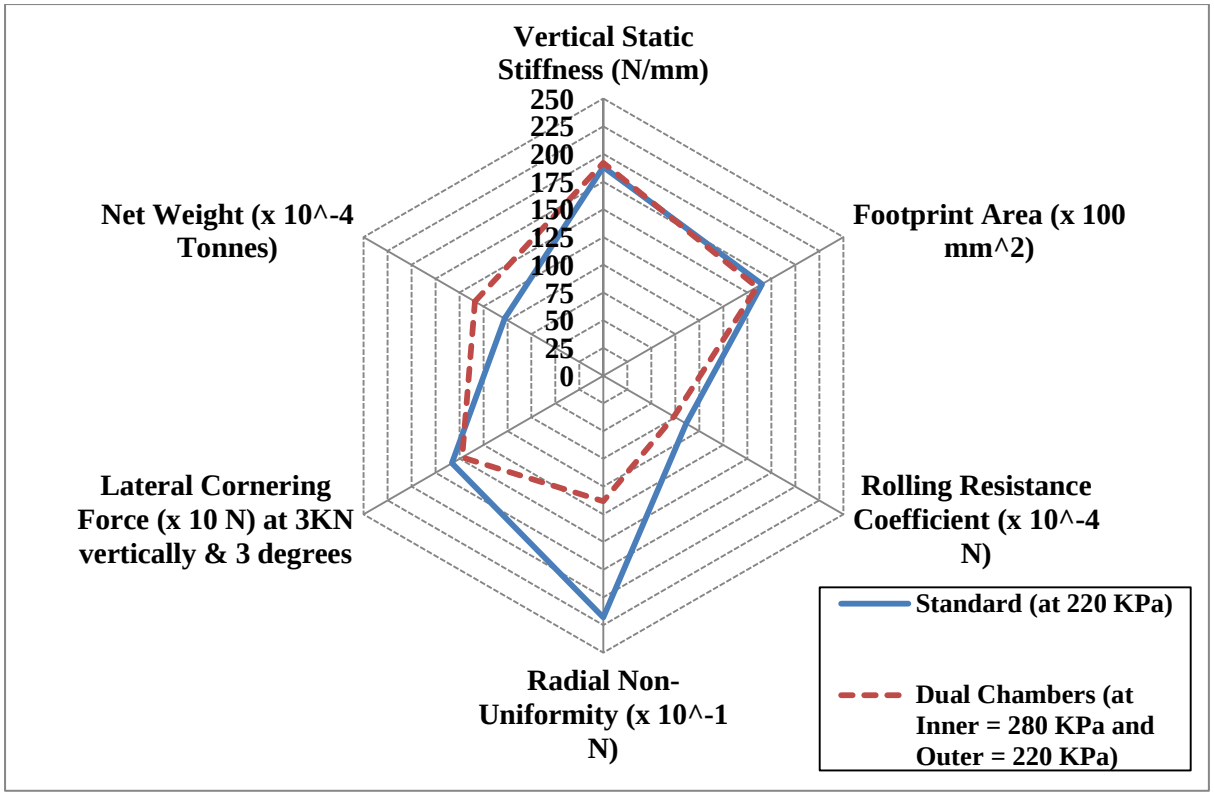

A) Rolling-Resistance and Other Features.

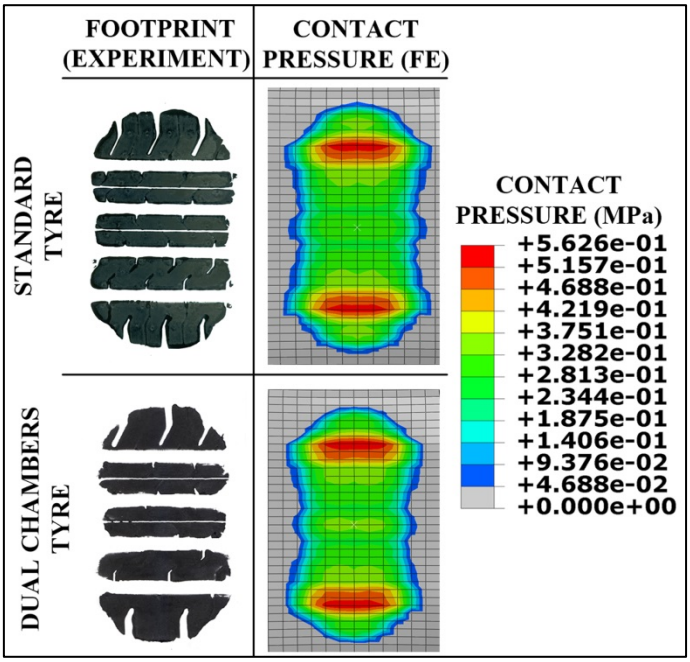

B) Contact-Patch.

Figure 7. Standard and Dual-Chambers Tires Characteristics for Straight Free-rolling (i.e., at 4 KN vertically and 30 Km/h)

The dual-chambers tire has slightly higher vertical stiffness than the standard tire which means it would maintain an almost similar level of mechanical comfort. However, a slightly smaller footprint is incurred, undermining the tire's gripping slightly, as the inner-chamber would help in pushing out the tread-center further circumferentially as seen in Table 4 and Figure 7 (B). As illustrated, the contact pressure distribution can be used as an approximation to the footprint shape since Abaqus/Explicit does not support a contact-patch area contour. The contact pressure pattern generated agrees with that of the literature [36-38]. During cornering, the dual-chambers demonstrated a marginal reduction in the lateral force which may undermine from the tire's grip and stability a little. These compromises can be negligible depending on the tire application. They can be addressed by lowering the outer-chamber's pressure a little further to gain the required tire's footprint and grip.

Another trade-off is the extra weight of nearly 3 Kg gained by the dual-chambers. This weight difference has almost no role to play on rolling-resistance within this paper's scope (i.e., straight free-rolling) since tire's rotational inertia would only noticeably affect rolling-resistance in traction-and-braking conditions agreeing with Walter [39]. Nevertheless, the net weight can be greatly reduced with proper designs, lightweight materials, or lighter wheels.

5. Multi-chambers Concept:

Based on the kinetic theory of gases, a gas is made-up of many tiny molecules that are arranged arbitrarily and far away from each other in a state of a continuous, fast and random motion in all directions. This makes the gas expandable to occupy the whole space of the container and compressible under loading. Furthermore, the gas pressure is established due to molecules' collisions against the container's walls.

For the standard tire, due to peristaltic pumping, a large portion of tire cavity's air will be experiencing repetitive expansion and compression. At expansion, from air-role perspective, cavity air will try to restore the tire's structure but after some delay (i.e., heat losses) due to the time taken for the required air-molecules to re-collide at the tire's inner-liner, reach equilibrium, and rebuild the necessary pressure to maintain the tire profile given the single bulky cavity volume and the randomness of the distant molecules' movement.

With the multi-chambers concept, this side-effect can be minimized by having the air-molecules confined in smaller cavity volumes shortening from the broadness and the time-taken for the air-molecules movement across the cavity space. Also, by manipulating and increasing the air concentration in certain volumes, it is possible to minimize the tread deformation through increasing the tire's overall stiffness and limiting the tread's curvature deformation.

In this context, three novel multi-chambers designs were developed, in Figure 8, as a part of a postgraduate research project on "Tyre Design and Analysis for low rolling-resistance". These designs were developed having different methods of relating the chambers' inner-walls to the main tire structure to investigate their effects on the tire's performance. In addition, the designs were set to meet a number of fundamental safety and operational requirements like:

- Allows for tire installation/removal to/from wheel rim.
- Contains a bead-lock chamber (i.e., zone (1)) set at the highest pressure to secure beads seating, maintain operation at run-flat, and support the other subsequent chambers.
- At least 35 KPa gap exists between the consecutive inner-chambers vertically starting with the bead-lock chamber, having the highest inflation, down to the tread

respectively to avoid undesired wrinkling and violent distortions in the inner-chambers profile [16].

- No perfectly straight and vertical inner-walls in direct contact with the tread to avoid a permanently stiffer tire at the expense of cushioning.
- No tiny or complex chamber(s) that would undermine from the design's manufacturability, functionality, and accommodation.

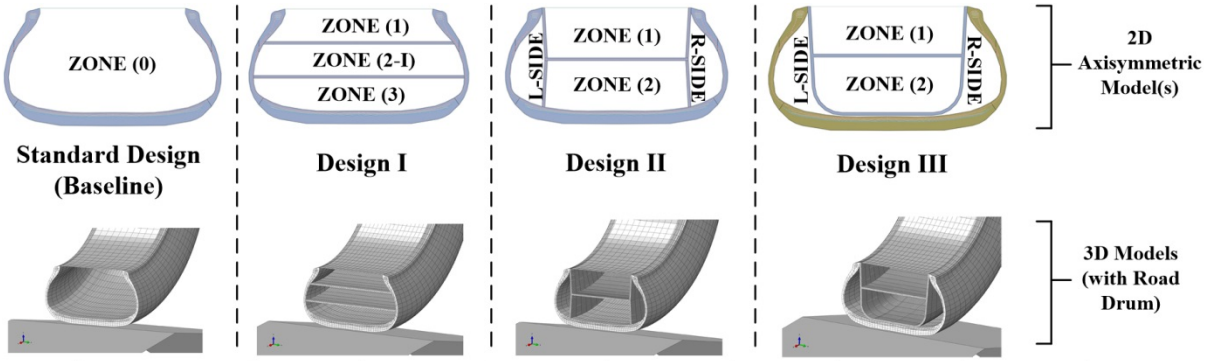

Inflation Mode	Zone (0)	Zone (1)	Zone (2)	Zone (2-I)	Zone (3)	L-Side	R-Side
Normal	220 KPa	320 KPa	220 KPa	280 KPa	220 KPa	220 KPa	220 KPa
Economy	280 KPa	320 KPa	280 KPa	280 KPa	245 KPa	220 KPa	220 KPa

Figure 8. Novel Multi-Chambers Designs.

The tire will be inflated at normal mode, as in Figure 8, to satisfy driving situations like acceleration, braking, bumpy-road rolling, and turning where grip and cushioning are emphasized. Furthermore, in the normal mode, the chamber's zone (i.e. zones (2), (3), L-Side and R-Side) in direct support of the tread profile is set at the same inflation pressure as the standard tire for comparison purposes and to evaluate the role of chambers' structural design. If grip and cushioning are not emphasized, like driving in straight flat-path with marginal acceleration and braking, the tire will be inflated at economy mode for enhanced vertical stiffness and lower rolling-resistance.

The three multi-chambers designs will be assessed against the “standard design” using the experimentally validated FE modeling earlier. The assessment will involve running all designs under straight and steady-state free-rolling at 4 KN vertical load, 30 Km/h rolling-velocity, and two different inflation settings (i.e., normal and economy modes). All designs will have “cornering” run at normal mode, slip angle of 3 degrees, 4 KN vertical load, and 10 Km/h rolling-velocity. From those runs, all designs will be evaluated for rolling-resistance, non-uniformity, mechanical comfort, cornering and grip.

6. Results and Discussions:

Under both normal and economy modes, in Figure 9, the rolling-resistance performance revealed that “design II” is the most energy-efficient design compared to the other designs with a rolling-resistance reduction of over 40% compared to the standard tire. This is because “design II” provides the highest vertical stiffness with the lowest profile fluctuation during rolling which makes it the least deformable as can be seen from the tire’s vertical deflection and the tread’s curvature deformation (i.e., footprint width) in Table 5. For an isothermal process and based on the first law of thermodynamics, less deformation would mean less work needed to restore that deformation and hence less energy consumed.

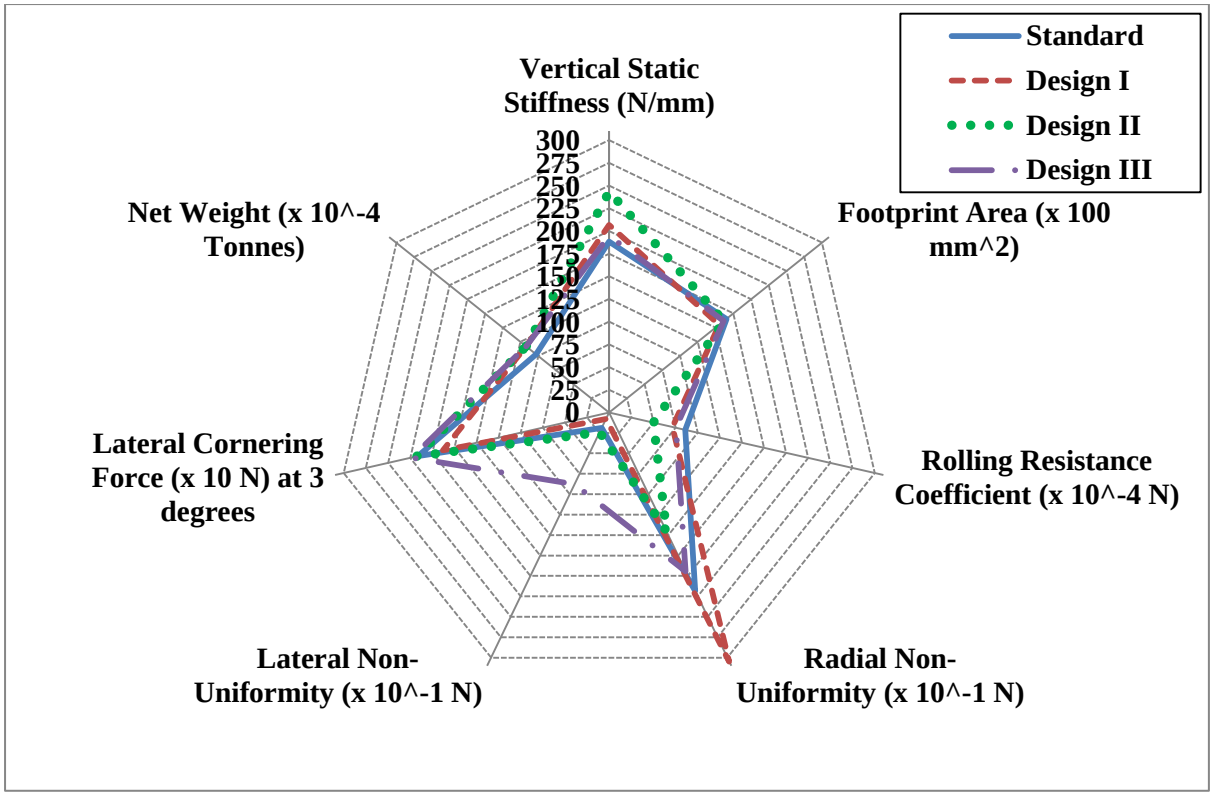

A) Performance at Normal Mode.

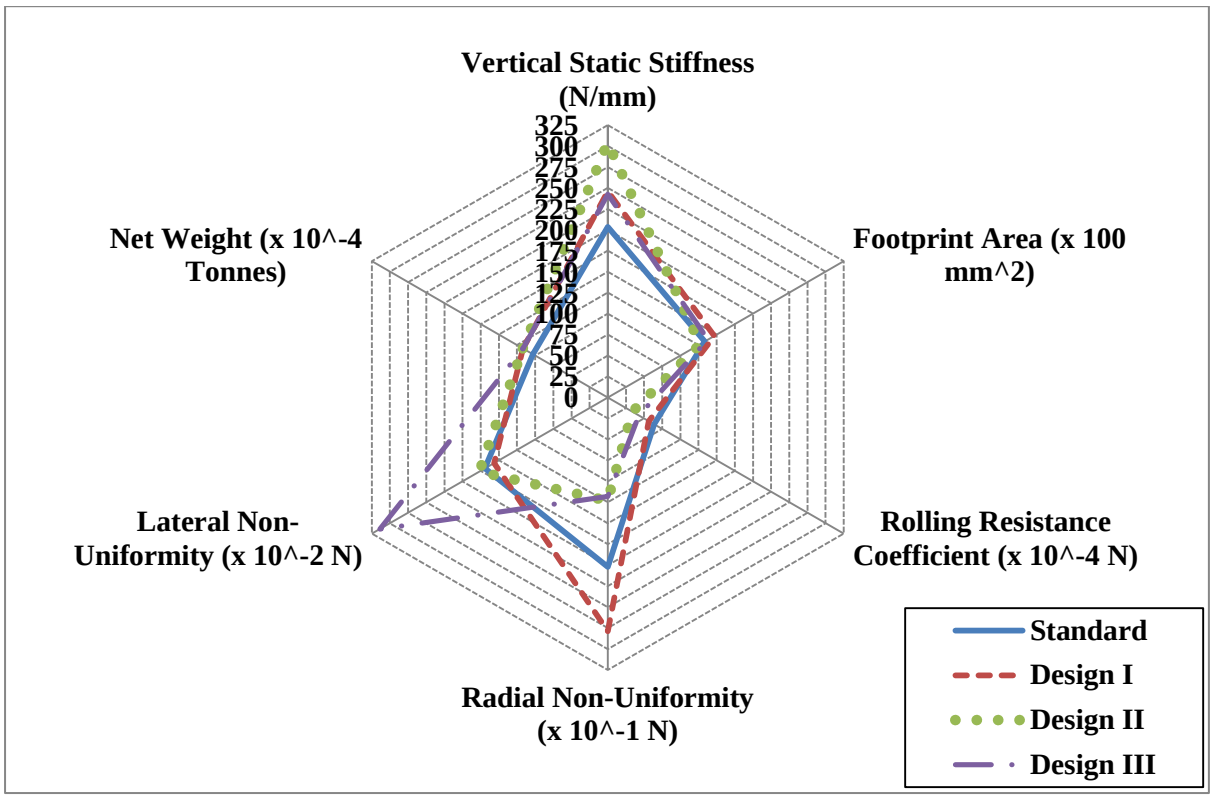

B) Performance at Economy Mode.

Figure 9. Performance Metrics of Multi-Chamber Designs.

Table 5. Footprint's Width and Vertical Deflection.

	Inflation Mode	Standard Design	Design I	Design II	Design III
Footprint Width (mm^2)	Normal	173.8245	180.197	171.638	169.9675
	Economy	165.872	178.9982	155.608	165.676
Vertical Deflection (mm)	Normal	21.264	19.367	16.431	20.540
	Economy	19.646	16.265	13.175	16.501

Such a performance can be related due to the level of the structural support and how effectively the air volume is being employed in each design to maintain the tire profile. The improved stiffness and the minimized deformational scale, as seen in tire's non-uniformity, in "design II" were gained through having additional inner sidewalls to assist the main sidewalls in withstanding the vertical loading and separate them from the main air cavity chambers (zones (1) and (2)) to avoid losing the bulk air volume supporting and maintaining the tire's tread profile. Those inner sidewalls were supported by a mid-circumferential inner-wall to hold them in position and help restrict air bulk movement. A clear example on the effectiveness and role of cavity design is the comparison between "design II" and "design III" at the normal mode where both designs have the same inflation pressure in all zones, yet they exhibit significantly different performances.

Table 6. Contact-Pressure Distribution.

	Normal Mode				
	Standard Design	Design I	Design II	Design III	
Contact Pressure (MPa)	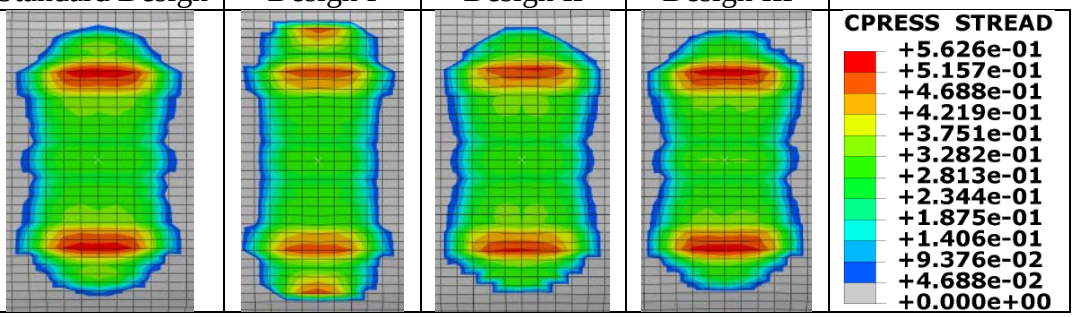				

Concerning tire's grip, both footprint area and contact pressure were looked at in Figure 9 (A) and Table 6 in the normal mode as key components that form the tire's grip mechanism [40]. A certain balance is needed to be preserved between the level of the contact pressure against that of the footprint area to prevent undermining the tire's grip [41].

At the normal mode, both "designs II and III" shared almost the same footprint area, contact-patch shape, and contact pressure pattern as the "standard design" with marginal differences. Such outcomes should keep the tire's grip in "designs II and III" at a close level to that of the "standard design". However, "design I" illustrated an odd contact-shape, different contact pressure pattern, and lower footprint area undermining from the tire's grip due to the design's sidewalls irregular outline and rigidity as will be indicated later.

For the radial non-uniformity, in Figure 9, under both normal and economy modes, "design I" has the highest non-uniformity during rolling followed next by the "standard design" while "design II" has the best uniformity and stable ride. In the lateral non-uniformity, under both normal and economy modes, "design III" had the most vibratory rolling while the rest of the designs had almost the same vibrational level.

The clear difference in the rolling non-uniformity between the designs is referred due to the stability of the inner-chambers and their air volumes, the chambers' support/interaction with the tire's profile and the tire sidewalls' flexibility. "Design I" had its inner-chambers walls integrated to the tire's sidewalls structure making them less flexible with an irregular outline, as shown in Figure 10. This sidewall irregularity would agitate and destabilize the air volume more agreeing with Schuring et al. [42] findings. Having a single large cavity, the "standard

design" had the most arbitrary and large movement of air volume across the cavity with the widest sidewall side movement as indicated in Figure 10. This goes in line with Schuring et al. [42] work too.

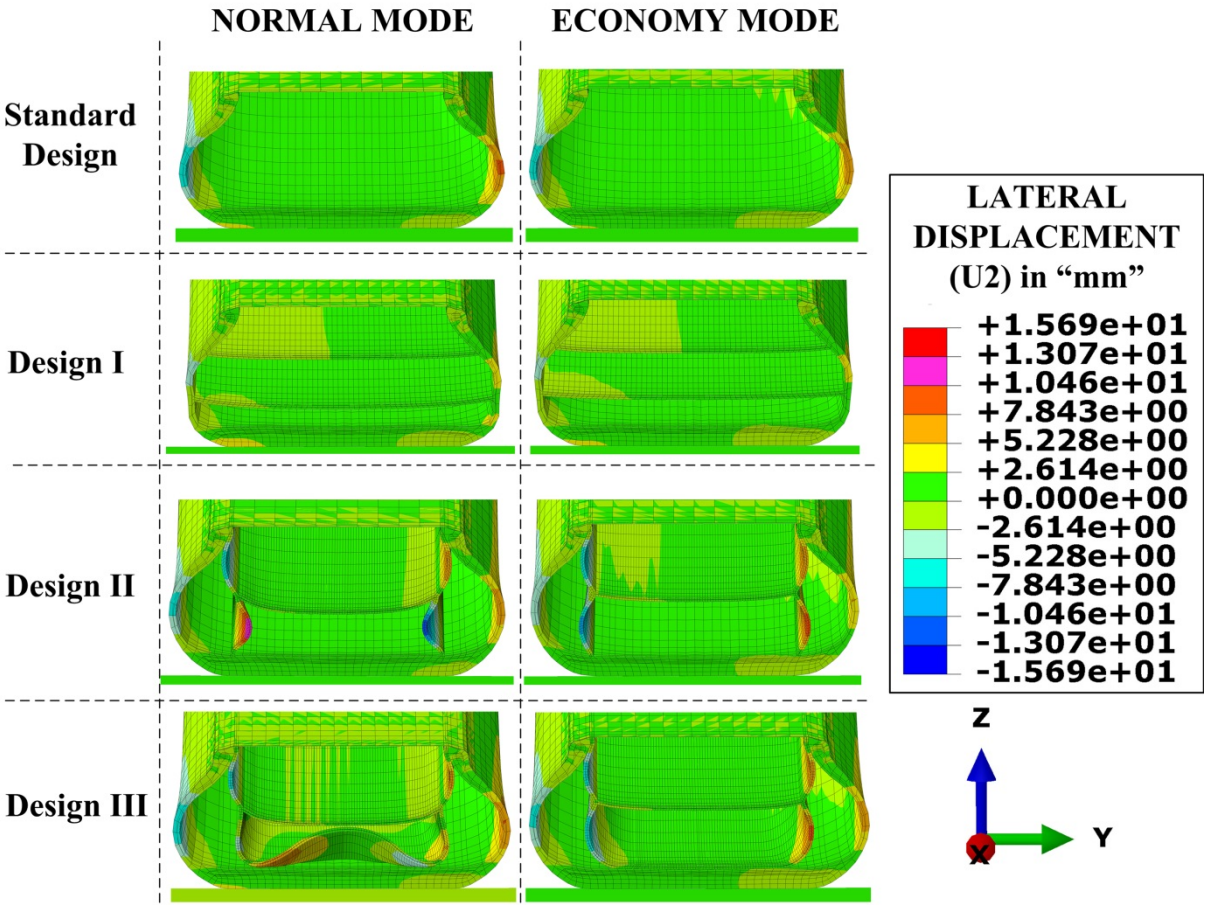

Figure 10. Deformed Tire's Profile under Vertical Loading.

With "design II", the large air volume and its random (long) movements were greatly reduced along with the interaction between the main air volume (zones (1) and (2)) and the main sidewalls by separating them into different confined cavity chambers while maintaining the main sidewalls flexibility and profile. This is because the air volume close to the sidewalls would experience more agitated and wild movements at higher rates than at the cavity center due to sidewall's curvy shape and movements. Schuring et al. [42] with Rae and Skinner [43] highlighted such behavior as well. Due to being detachable, "design III" inner-chamber (zone

(2)) would suffer from instability, excess non-uniform deformation and side-sliding, as a result of random air shifts, when subjected to peristaltic pumping during rolling especially at the normal mode as illustrated in Figures 9 and 10.

For the mechanical comfort at the normal mode, based on the vertical stiffness, “design II” is the stiffest with 243 N/mm while the “standard design” being the least stiff with 188 N/mm. This would undermine from “design II” ride comfort to an extent. Depending on tire application, it might be of acceptable comfort level since the common vertical stiffness for radial passenger-car tires is around 200-220 N/mm [31, 44-46]. If the tire’s mechanical comfort was case-sensitive; the available alternatives to improve tire’s cushioning would be to rely on vehicle suspension compensation, reduce the inflation-pressure(s), and modify inner-chambers for thinner inner-walls or different inner-wall’s orientation.

The multi-chamber designs are estimated to have an extra weight of around 1.42 Kg over the “standard design” based on a weighted section of the standard tire’s sidewall which the chambers are made of. The weight improvements and its role on rolling-resistance are outside this paper’s scope as illustrated previously.

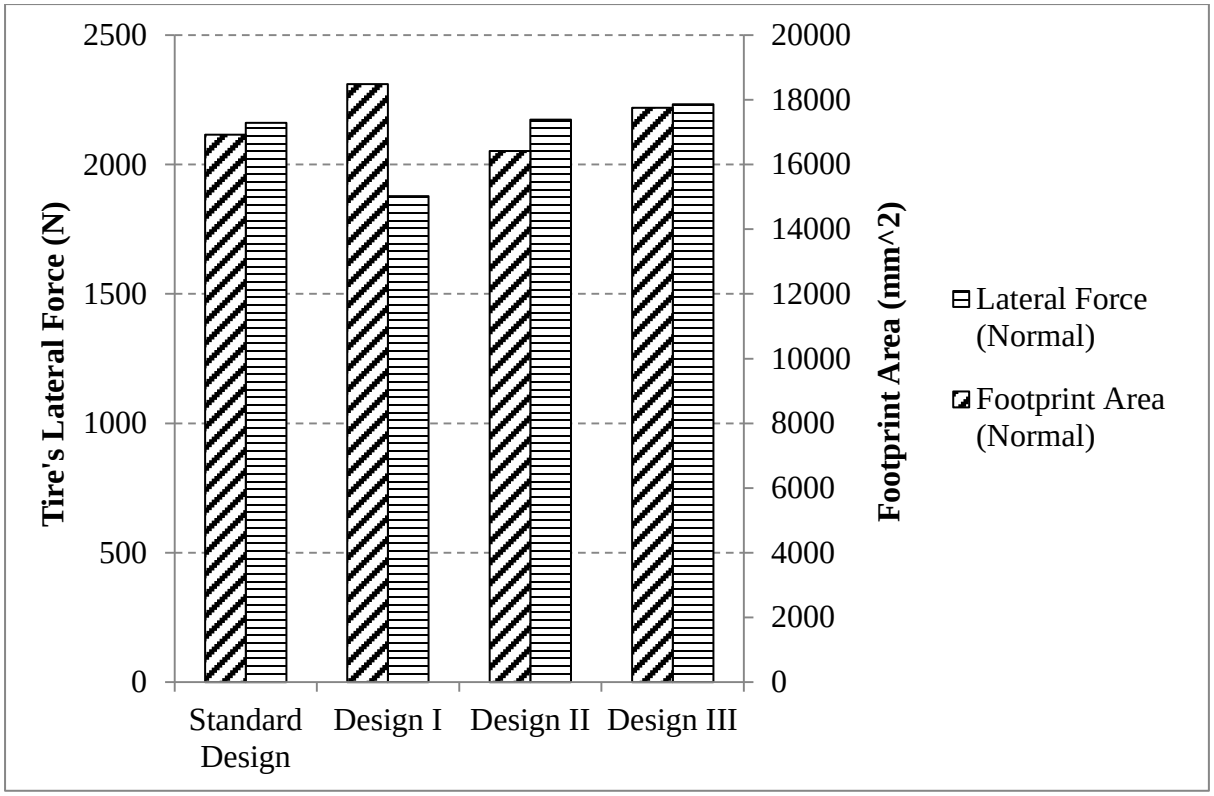

Figure 11. Cornering Characteristics.

For cornering, in Figure 11, “design II” and “design III” showed similar performance as that of the “standard design” regarding tire’s lateral force and contact-patch area. This reveals the capability of “design II” to maintain the vehicle’s stability during cornering. However, for “design III”, the tire’s stability is undermined by the excess non-uniform deformation of zone (2) chamber and throughout the whole tire. In “design I”, the tire’s stability is also undermined but by the sidewall’s inflexibility and irregularity which caused vibratory roll and lower lateral force.

7. Conclusion:

The multi-chambers cavity tire is found to be an immature research field at its beginnings with little research findings. This concept was further investigated, and the following main outcomes were reached:

- In FE modeling, the usage of the distributed pressure loading was found ineffective in accounting for air/structure interaction in multi-chambers tires.
- Considering the tire's cavity air as fluid-filled cavity volume(s) in FE is found to be a valid alternative to account for the global air/structure interaction.
- The tire's deformation and flexibility are affected by the inner-chambers' structural set-up in relation to the tire's, how it controls the global air movement to maintain the tire profile, and air concentration inside the chamber(s).
- Isolating the air cavity volumes of the tire's sidewalls from that of the tread would significantly help in stabilizing the global air volume maintaining the tread's profile while sustaining the sidewalls' flexibility and shape.
- Smaller air cavities would mean quicker recovery of air volume after tire deformation at the contact-patch.
- Tire's rolling vibrations depends on the stability of the inner-chambers and its cavity air, the regularity of the tire's profile and the tire sidewalls' flexibility.
- "Design II" is the best choice for low rolling-resistance (i.e., with a reduction of over 40%) while maintaining a close level of tire's grip and corner-handling but lowered cushioning to an extent compared to the "standard design".
- Both "designs I and III" had problems related to stability and non-uniformity although they had lower rolling-resistance than the "standard design" but higher than "design II".

In overall, the multi-chambers tire is found to be a good alternative solution to reduce the rolling-resistance substantially with minimum compromise to the other essential tire's features like grip, mechanical comfort, and cornering.

8. Future Work:

"Design II" needs further characterization and optimization to reach a more tailored and balanced tire design for rolling-resistance, grip and mechanical comfort. This may involve further investigating design parameters like weight, chamber(s) layout, cavity volume, and inflation pressure for optimum settings.

Also, the design's manufacturability needs to be looked at to assess its feasibility. A potential manufacturing choice would be using "fabric calendaring" to produce the multi-chamber inner-walls separately and then "multi-stage curing" to join the chambers' inner-walls to the tire's inner liner starting from the innermost to the outermost contact-points respectively.

Conflict of Interest:

'The Author(s) declare(s) that there is no conflict of interest'

9. References:

[1] Aldhufairi HS, Olatunbosun OA. Developments in tyre design for lower rolling resistance: a state of the art review. Proceedings of the Institution of Mechanical Engineers, Part D: Journal of Automobile Engineering. 2017.

[2] Jae E. Data directory: future market insights on specialty silicas. Tire Technology International. 2015:70.

[3] LaClair T. Rolling resistance. The pneumatic tire, National Highway Traffic Safety Administration, US department of Transportation, Washington DC. 2006:475-532.

[4] Hall G, inventor; Fusion Innovations Ltd assignee. Pneumatic Tyre with Multiple Chambers patent WO2014057282A1. 2014.

[5] Rodenbeck PD, inventor; Toyota Motor Corp, assignee. Magneto-rheological elastomer wheel assemblies with dynamic tire pressure control patent US8176958B2. 2012.

[6] Howard FA, inventor; Frank A Howard assignee. Safety pneumatic tire patent US2969824A. 1961.

[7] Kenneth K, Brook O, inventors; Eng K. Kenneth assignee. Multi-chamber safety tire patent US20030131918A1. 2003.

[8] Mazhar MS, inventor; US Secretary of Army, assignee. Multi-chamber pressurizable tube for a tire patent US6076580A. 2000.

[9] Seyed K, inventor; Khalil Seyed assignee. Tire patent US2525752A. 1950.

[10] Huber VR, inventor; Uniroyal Goodrich Tire Co, assignee. Tire patent US3487870A. 1970.

[11] Cupp HN, inventor; Harry N Cupp, assignee. Automobile tire patent US1989402A. 1935.

[12] Mclean WD, inventor; Willard D. McLean, assignee. Supplemental Shoe for Automobile Tires patent US2735471A. 1956.

[13] Mcleod NW, inventor; Norman W Mcleod assignee. Multi-chambered vehicle tire patent US2780266A. 1957.

[14] Francesco M, Maria M, Marina M, inventors; Curtiss-Wright Corp, assignee. Tire for vehicles, composed of two concentric annular chambers patent US2925845A. 1960.

[15] Lambe DM, inventor; Lambe Donald M assignee. Dual-chamber pneumatic tire patent US4293017A. 1981.

[16] Coyote. Coyote Boltless Beadlock System Costa Mesa [19/09/2017]. Available from: https://www.coyoteents.com/beadlocks/.

[17] Evans R. Concept Tires: Future Proofs. Tire Technology International. 2015;3.

[18] Bridgestone. Multi-chamber tyre extends thinking on stability. European Automotive Design. 2006;10(5):12.

[19] Kubba AIS. Intelligent tyre technologies. Birmingham, UK: University of Birmingham; 2018.

[20] Wei C. A finite element based approach to characterising flexible ring tire (FTire) model for extended range of operating conditions [PhD]. Birmingham, UK: University of Birmingham; 2015.

[21] Aldhufairi HS, Essa K. Tire Rolling-Resistance Computation based on Material Viscoelasticity Representation. Advances in Automotive Engineering. 2018;1(2):167-83.

[22] Michelin. The Tyre: Mechanical and Acoustic Comfort: Société de technologie Michelin; 2002.

[23] Mawby WD, Sauls J, inventors; Michelin Recherche Et Technique, S.A.Societe De Technologie Michelin assignee. Improvement of tire uniformity through identification of process effects using singlet tire regression analysis patent WO2012002949A1. 2012.

[24] Ask T. Engineering for Industrial Designers and Inventors: Fundamentals for Designers of Wonderful Things: " O'Reilly Media, Inc."; 2016.

[25] Myers R. The basics of chemistry. London, UK: Greenwood Publishing Group; 2003.

[26] Zheng R, Li M, Wu B. Autoregressive Model for Automobile Tire Pressure and Temperature Based on MATLAB. In: Jin D, Lin S, editors. Advances in Computer Science and Information Engineering; Verlaf Berlin Heidelberg: Springer; 2012. p. 513-20.

[27] Yang X. Finite element analysis and experimental investigation of tyre characteristics for developing strain-based intelligent tyre system [PhD]. Birmingham, UK: University of Birmingham; 2011.
[28] Kim T-W, Kim H-H, Jeong H-Y, Park H-C, Kim Y-H, Choe J-H. Determination of Prony Series Parameters and Rolling Resistance Simulation of a Tire. In: Yao Z, Yuan M, Zhong W, editors. Sixth World Congress on Computational Mechanics in conjunction with the Second Asian-Pacific Congress on Computational Mechanics; Beijing, China. Beijing: Tsinghua University Press & Springer; 2004.
[29] Ghosh P, Saha A, Mukhopadhyay R. Prediction of tyre rolling resistance using FEA. Constitutive Models for Rubber. 2003:141-6.
[30] Wei C, Olatunbosun OA, Behroozi M. Simulation of tyre rolling resistance generated on uneven road. International journal of vehicle design. 2016;70(2):113-36.
[31] Lee C-R, Kim J-W, Hallquist JO, Zhang Y, Farahani AD. Validation of a FEA tire model for vehicle dynamic analysis and full vehicle real time proving ground simulations. SAE Technical Paper; 1997. Report No.: 0148-7191.
[32] Hoever C. The simulation of car and truck tyre vibrations, rolling resistance and rolling noise [Doctor of Philosophy]. Göteborg, Sweden: Chalmers University of Technology; 2014.
[33] Hernandez JA, Al-Qadi IL, Ozer H. Baseline rolling resistance for tires' on-road fuel efficiency using finite element modeling. International Journal of Pavement Engineering. 2017;18(5):424-32.
[34] Narasimha Rao K, Kumar RK, Bohara P. A sensitivity analysis of design attributes and operating conditions on tyre operating temperatures and rolling resistance using finite element analysis. Proceedings of the Institution of Mechanical Engineers, Part D: Journal of Automobile Engineering. 2006;220(5):501-17.
[35] Parisouz S. Experimental rubber friction modelling and its applications in tyre finite element analysis: University of Birmingham; 2018.
[36] Vayalat TM. Tire Contact Patch Characterization through Finite Element Modeling and Experimental Testing. Blacksburg, VA: Virginia Polytechnic Institute and State University; 2016.
[37] Yang X, Behroozi M, Olatunbosun OA. A neural network approach to predicting car tyre micro-scale and macro-scale behaviour. Journal of Intelligent Learning Systems and Applications. 2014;6(01):11.
[38] Kumar U, Goyal S, Unnikrishnan G, Thomas TK. Application Of Improved Simulation Approach For Tire Foot Print Contact Pressure Estimation. International Journal of Mechanical And Production Engineering. 2015;3(5):97-9.
[39] Walter J. Fuel economy and effective mass: The tire's place in fuel economy. Tire Technology International. 2016;3:16.
[40] Michelin. The tyre grip. Clermont–Ferrand, France: Société de Technologie Michelin 2001.
[41] Allen J. Jeep 4x4 Performance Handbook: MotorBooks International; 1998.
[42] Schuring D, Skinner G, Rae W. Contained Air Flow in a Radial Tire. SAE Transactions. 1981:705-12.
[43] Rae WJ, Skinner GT. Measurements of Air Flow Velocity Distributions Inside a Rolling Pneumatic Tire. SAE Technical Paper; 1984. Report No.: 0148-7191.
[44] KuliKowsKi K, Szpica D. Determination of directional stiffnesses of vehicles' tires under a static load operation. Eksploatacja i Niezawodność. 2014;16(1):66-72.
[45] Soltani A, Goodarzi A, Shojaeefard MH, Saeedi K. Optimizing tire vertical stiffness based on ride, handling, performance, and fuel consumption criteria. Journal of Dynamic Systems, Measurement, and Control. 2015;137(12):121004.
[46] Mhaske N, Narwade P, Nagarkar M. Stiffness Analysis of Passenger Car Tire Using Nitrogen. International Journal of Scientific and Research Publications. 2016;6(1):140-8.